Kolmogorov turbulence in a random-force-driven Burgers equation: Anomalous scaling and probability density functions

Alexei Chekhlov and Victor Yakhot
Program in Applied and Computational Mathematics, Princeton University, Princeton, New Jersey 08544
(Received 6 April 1995)

High-resolution numerical experiments, described in this work, show that velocity fluctuations governed by the one-dimensional Burgers equation driven by a white-in-time random noise with the spectrum $\overline{|f(k)|^2} \propto k^{-1}$ exhibit a biscaling behavior: All moments of velocity differences $S_{n\leq 3}(r)=\overline{|u(x+r)-u(x)|^n} \equiv \overline{|\Delta u|^n} \propto r^{n/3}$, while $S_{n>3}(r) \propto r^{\xi_n}$ with $\xi_n \approx 1$ for real $n>0$ [Chekhlov and Yakhot, Phys. Rev. E **51**, R2739 (1995)]. The probability density function, which is dominated by coherent shocks in the interval $\Delta u<0$, is $\mathcal{P}(\Delta u,r) \propto (\Delta u)^{-q}$ with $q \approx 4$. A phenomenological theory describing the experimental findings is presented.

PACS number(s): 47.27.Gs

Our recent study [1] of the one-dimensional Burgers equation

$$\frac{\partial u}{\partial t}+u\frac{\partial u}{\partial x}=f+\nu\frac{\partial^2 u}{\partial x^2} \tag{1}$$

driven by a white-in-time random force defined by the correlation function

$$\overline{f(k,t)f(k',t')} \propto D(k)\delta(k+k')\delta(t-t') , \tag{2}$$

with $D(k)=\epsilon_0 k^{-1}$ and $\epsilon_0=O(1)$, was motivated by an interest in dynamical processes which involve an interplay between chaotic and coherent phenomena. It has been shown that the velocity field $u(x,t)$ consists of random-in-time and random-in-space fluctuations superimposed on the relatively strong and long-living shocks. Numerical simulations yielded the energy spectrum $E(k) \propto \overline{|u(k)|^2} \propto k^{-x}$ and $x=\frac{5}{3}\pm 0.02$, characteristic of Kolmogorov turbulence [2] and the Eulerian correlation function $C(k,\omega)=\overline{|u(k,\omega)|^2} \propto k^{-7/3}\Phi(\omega/k^z)$ with the dynamic exponent $z=\frac{2}{3}$. This result shows that in this system the kinematic transport of the small-scale velocity fluctuations by the large-scale structures is very weak. Investigation of the velocity structure functions $S_n(r)=\overline{[u(x+r)-u(x)]^n} \equiv \overline{(\Delta u)^n}$ with integer n revealed strong deviations from the Kolmogorov picture of turbulence: all moments $S_{n>3}(r) \propto r^{\xi_n}$ with $\xi_n \approx 1$, characteristic of strong shocks. Thus the system governed by (1) and (2) shows both "normal" (Kolmogorov) and anomalous scalings with the latter dominated by the coherent structures (shocks). In this work we are interested in the details of the probability density functions (PDF's) characterizing the fluctuations generated by (1) and (2) and in the role the structures play in the determination of the PDF's shape. The PDF $\mathcal{P}(\Delta u,r)$ is defined such that $\mathcal{P}(X,r)dX$ is the probability of finding a velocity difference $\Delta u=u(x+r)-u(x)$ within the interval $(X,X+dX)$ for infinitesimally small dX. A spectral code with 12 288 Fourier modes was used in the numerical experiment. Equation (1) with a hyperviscous (instead of viscous) dissipation term was solved. The details of the numerical procedure are reported in [1].

The most prominent feature of the Burgers equation is a tendency to create shocks and, consequently, to increase the negative velocity differences $\Delta u<0$ and to decrease the positive ones $\Delta u>0$ [3]. Thus strong asymmetry of the curve $\mathcal{P}(\Delta u,r)$ is expected. The two-point PDF $\mathcal{P}(\Delta u,r)$ was measured for a set of separations r covering a variety of scales in the system in the following way. The range of variation of the velocity difference, $-5<\Delta u/u_{\rm rms}<5$, was divided into 10^4 bins. The data were collected during a time longer than the ten largest eddy turnover times [corresponding to $O(10^7)$ time steps] and were distributed among the appropriate bins to generate a histogram. Figure 1 presents $\mathcal{P}(\Delta u,r)$ for the inertial range separations $r/dx=200,250,300,350,400$, where $dx=L/12\,288$ is the mesh size and $L=2\pi$ is the system size. If follows from (1) and (2) that $(\Delta u)^3 \propto \epsilon_0 r \ln(rk_d)$ and that is why this PDF has a

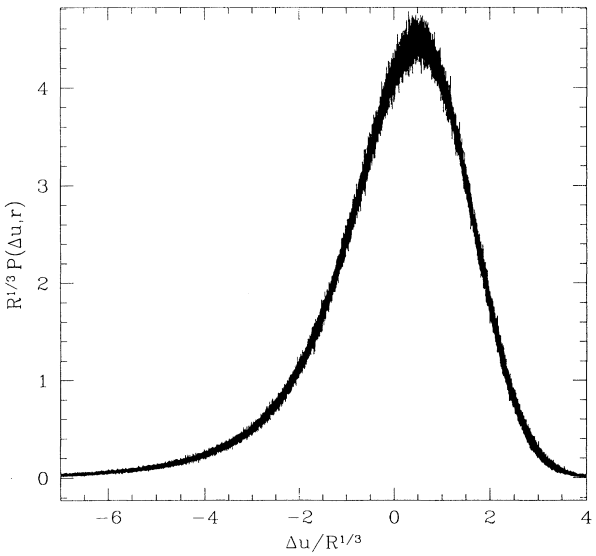

FIG. 1. Normalized two-point PDF $F(\Delta u/R^{1/3})=R^{1/3}\mathcal{P}(\Delta u,r)$ for separations $r/dx=200,250,300,350,400$ within the universal range. The collapse of various curves supports the choice of the scaling variable $\phi=(\Delta u)/R^{1/3}$, where function $R(r)$ is defined in the text.

shifted maximum, approximately at $\phi=(\Delta u)/R^{1/3} \approx 0.5$. Here the function $R(r)$ defined as $R(r)\equiv\int[f(x+r)-f(x)]^2dx$ was also directly measured. It is fully force dependent and in a system with viscosity it may be analytically calculated for the inertial-range values of separation r, giving $R(r)\propto\overline{(\Delta u)^3}\propto\epsilon_0 r\ln(rk_d)$, where $k_d\to+\infty$ is a dissipative cutoff wave number. Technically speaking, the system considered in this work does not have a real "inertial range" since the mean dissipation rate $\bar{\epsilon}=O(\epsilon_0\ln(Lk_d))$ depends on the ultraviolet cutoff k_d. This dependence, however, is weak and in what follows we take $k_d=O((\epsilon_0/\nu^3)^{1/4})$.

The tail of the PDF $\mathcal{P}(\Delta u,r)$ for $\Delta u<0$ is shown in Fig. 2 for various magnitudes of the displacement r in the universal range. One may observe from this figure that the PDF for $\Delta u<0$ may be well approximated as

$$\mathcal{P}(\Delta u,r)\propto(\Delta u)^{-q}\ , \tag{3}$$

with $q\approx 4$. We have also found that $\mathcal{P}(\Delta u,r)$ for $\Delta u>0$ is well fitted by the exponential

$$\mathcal{P}(\Delta u,r)\propto e^{-\alpha(\Delta u)^3/r}\ , \tag{4}$$

with the constant α to be determined from the theory. The dynamic argument leading to (3) will be presented below. The results in Figs. 1 and 2 are highly nontrivial because the observed algebraic decay of the PDF $\mathcal{P}(\Delta u,r)$ as $\Delta u/(\Delta u)_{rms}\to-\infty$ leads to the divergence of the moments $S_n(r)$ for $n>3$ for the inviscid case. However, as we also observed, the single-point PDF $\mathcal{P}(u)$ is a very rapidly decreasing function which is close to the Gaussian and that is why the occurrence of shocks with an amplitude $\Delta u>U_0\approx[\bar{\epsilon}L\ln(Lk_d)]^{1/3}$ is highly improbable and one can expect the PDF $\mathcal{P}(\Delta u,r)$ to decrease sharply for $\Delta u<-U_0$. This is sufficient for the existence of all moments $S_n(r)$. A full analytical theory leading to an expression for $\mathcal{P}(\Delta u,r)$, which unifies both asymptotics (3) and (4), is planned to be published elsewhere [4].

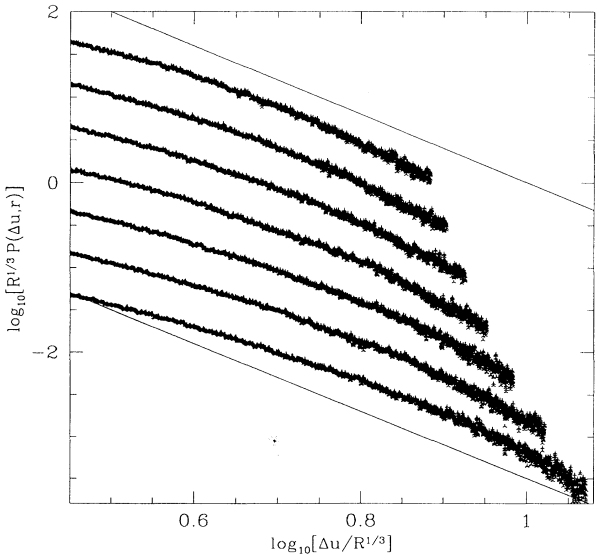

FIG. 2. The tail of the two-point PDF $\mathcal{P}(\Delta u,r)$ (points) for separations $r/dx=150,200,250,300,350,400,450$ within the universal range, plotted on a logarithmic-logarithmic scale. The slope of the solid lines is equal to -4. The graphs for different values of r are arbitrarily shifted along the vertical axis for clarity.

To develop a phenomenological theory we assume that the flow can be represented as a superposition of coherent and random components. The coherent contribution is visualized as a "gas of shocks" and a single structure (shock) can be approximated by the exact tanh solution of the unforced problem [3]. In particular, let us assume that the solution for the normal (not the hyper) viscosity case has the form

$$u(x,t)=-\sum_{i=0}^{N}U_i\tanh\left[\frac{(x-a_i)U_i}{2\nu}\right]+\phi(x,t)\ . \tag{5}$$

The first contribution to the right side of (5) describes the slowly varying coherent "gas of shocks," whereas the second represents the effects unaccounted for by the first term. Here a_i and U_i denote the coordinates of the centers of the shocks and the shock amplitudes, respectively. The physical picture behind this representation is the following: the forcing produces the low energy excitations which coagulate into ever stronger well-separated shocks due to the nonlinear interactions. It will be clear below that the detailed shape of the shock assumed in (5) is unimportant. The most essential feature of the tanh solution (5) is that the shock width $l_i\approx\nu/U_i$, which means that the stronger the shock, the more narrow it is.

Statistics of the dissipation rate fluctuations were investigated in detail in Ref. [1]. It has been shown that the energy dissipation takes place mainly ($\approx 99\%$) inside the well-separated strong shocks. Thus it follows from (5) that the dissipation rate in interval of length r is

$$\epsilon_r=\frac{1}{4r\nu}\int_{x=0}^{r}dx\sum_{i,j=0}^{N}\frac{U_i^2U_j^2}{\cosh^2Y_i\cosh^2Y_j}\ , \tag{6}$$

where we denote $Y_i=(x-a_i)U_i/(2\nu)$. The principal contribution to the sum comes from the strong and narrow shocks, and therefore we can neglect the nondiagonal terms with $i\neq j$. Assuming the density of the shocks to be r independent we have

$$\epsilon_r\propto\sum_{i=0}^{N}\frac{U_i^3}{r}\approx\frac{\overline{U^3}}{r}\ . \tag{7}$$

On the other hand, it can be directly shown from (1) and (2) that

$$\epsilon_r=\epsilon_0\ln\left[\frac{LU_0}{\nu}\right]\ . \tag{8}$$

Introducing the PDF $\mathcal{P}(U,r)$ to find a shock with amplitude U in the interval of the length r we obtain from the last two relations

$$\int_{\nu/L}^{U_0}U^3\mathcal{P}(U,r)dU\propto\epsilon_0 r\ln\left[\frac{LU_0}{\nu}\right]\ , \tag{9}$$

from which we readily establish the form of $\mathcal{P}(U,r)$,

$$\mathcal{P}(U,r) \propto \frac{\epsilon_0 r}{U^4} . \tag{10}$$

Since $\mathcal{P}(U,r)=\mathcal{P}(U)r/L$, the relation (10) establishes the shape of PDF $\mathcal{P}(U) \propto U^{-4}$ to find a shock of the amplitude U. Note that r/L is the probability to find a shock center within the interval of the length r which is in turn placed in the larger interval of the length L. The low integration limit ν/L corresponds to the amplitude of the "weakest structure," contributing to ϵ_r. Formula (10) is a consequence of relations (7) and (8), and is valid in the logarithmic case when the forcing function is defined by (2). It is only in this case that we can establish the form of the PDF.

Thus, according to the data presented in Fig. 1 and the theoretical considerations developed above, the PDF of velocity differences can be represented as

$$\mathcal{P}(\Delta u,r)=aR^{-1/3}F\left[\frac{\Delta u}{R^{1/3}}\right] \tag{11}$$

in the interval $O(-1)<x\equiv\Delta u/R^{1/3}<\infty$, where function $R(r)$ is defined above, a is a numerical constant, and $F(x)$ is a scaling function (see [5]) which is assumed to go rapidly to zero when $|x|$ is large. In the interval $x \ll -1$, and $|\Delta u|<O(U_0)$, where the PDF is dominated by the well-separated shocks, we have

$$\mathcal{P}(\Delta u,r)=b\frac{\epsilon_0 r}{(\Delta u)^4} , \tag{12}$$

where b is a numerical constant. When $\Delta u \ll -U_0$, the PDF is a rapidly decreasing function of $\Delta u/U_0$. The moments of velocity difference are evaluated readily with the result

$$S_n(r)=\int(\Delta u)^n\mathcal{P}(\Delta u,r)d\Delta u$$
$$=br\epsilon_0\frac{U_0^{n-3}-(\epsilon_0 R)^{n/3-1}}{n-3}+B_n(\epsilon_0 R)^{n/3} , \tag{13}$$

where the amplitudes B_n depend on the shape of the scaling function $F(x)$. The constants $B_n \propto (-1)^n$ for integer n and for the noninteger values of n the structure functions $S_n=\overline{|\Delta u|^{(n)}}$ so that relation (13) should include the absolute value of the first term on the right side. It follows from (11)–(13) that all moments $S_n(r)$ with $n>3$ are completely determined by the upper cutoff in (13),

$$S_n(r) \propto \epsilon_0 r\frac{U_0^{n-3}}{n-3} , \tag{14}$$

which is in excellent quantitative agreement with [1], whereas for $0 \le n \le 3$

$$S_n(r) \propto (\epsilon_0 R)^{n/3} , \tag{15}$$

as in the Kolmogorov theory of turbulence [2]. Thus the anomalous scaling of the velocity structure functions $S_n(r)$ appears only for $n>3$. It should be stressed that, in accord with (13), in the logarithmic case considered in this work the contribution from the shocks to the moments $S_{n<3}$ is smaller than the one from the scaling component of the PDF only by a factor of $1/\ln(rk_d)$, which makes the experimental investigation of the details of the crossover very difficult.

The prediction (13) has been tested in [1]. It has been shown that $S_{2n}(r) \propto r^{\xi_{2n}}$ with $\xi_{2n} \approx 0.91$ for $n>2$, indicating that these correlation functions are dominated by coherent shocks. The results of the measurements of the structure functions $S_n(r)$ with $n=\frac{1}{3},\frac{2}{3},\ldots,\frac{6}{3}$, presented in Fig. 3, are in good agreement with the scaling law (15). The general structure of the moments of velocity

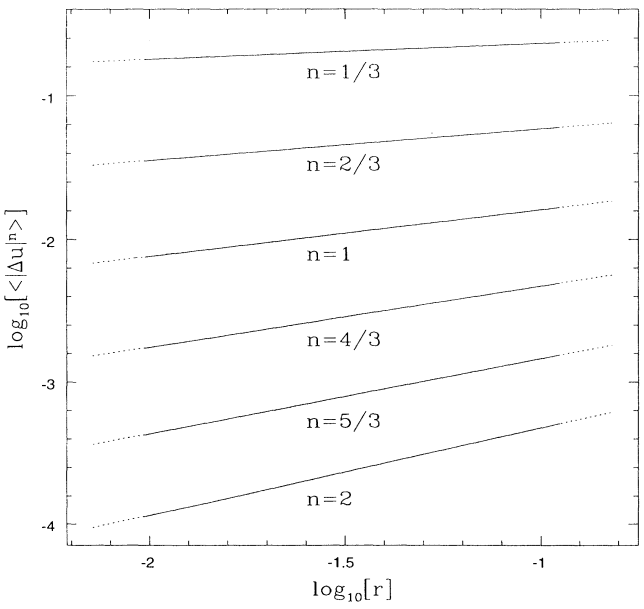

FIG. 3. Velocity structure functions $\overline{|\Delta n|^n}$ for noninteger values $n=\frac{1}{3},\frac{2}{3},\ldots,\frac{6}{3}$ (dotted curves). Slopes of the linear least-squares fits (solid lines) from top to bottom, respectively, are 0.111, 0.222, 0.330, 0.433, 0.531, and 0.620.

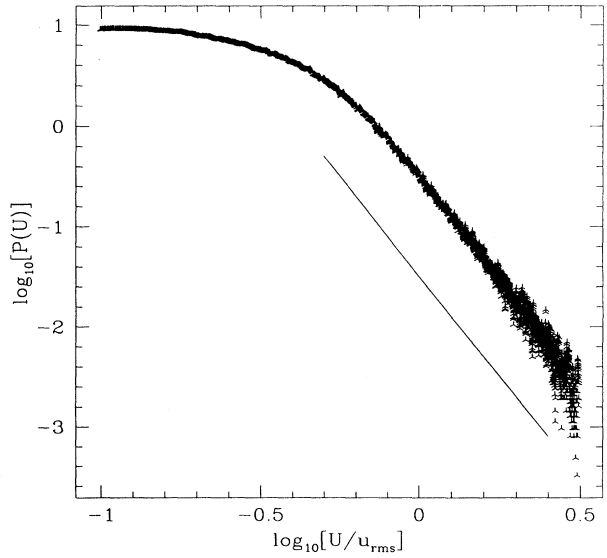

FIG. 4. PDF of shock amplitudes, $\mathcal{P}(U)$ on a logarithmic-logarithmic scale (points). The slope of the solid line is equal to -4.

differences given by expressions (13)–(15) is similar to the outcome of the recent theories of the random-force-driven Burgers equation by Polyakov [4] ($1d$) and Bouchaud, Mézard, and Parisi [5] ($d \to \infty$). The Polyakov theory confirmed our qualitative argument leading to the algebraic decrease of the PDF in the interval $\Delta u < 0$.

Figure 4 presents the PDF of the shock amplitudes. The problem of the shock location was solved in the following simple but reliable way. At each spatial point x the local gradient of the solution $u(x)$ was measured. Then, if $u'(x) \geq 0$, it was assumed that this point x is outside of a shock, otherwise x lies inside of a shock. Once inside a shock, one can march in x until the gradient becomes zero, and thus the boundaries of the shock may be located, and so forth. Note that the shock amplitude obtained in this way has been corrected to exclude the Gibbs phenomenon typical in spectral approximations of discontinuous functions. To reduce the statistical noise in $\mathcal{P}(U)$ in Fig. 4, a simple smoothing procedure was applied: $\mathcal{P}(U)$ was averaged over eight surrounding points. The result presented in Fig. 4 demonstrates that

$$\mathcal{P}(U) \propto U^{-4} \tag{16}$$

is observed for all $|U/U_{\rm rms}| > 0.5$. The fact that $\mathcal{P}(\Delta u) \approx \mathcal{P}(U)$ when $\Delta u < 0$ tells us that in this range $\mathcal{P}(\Delta u)$ is dominated by the well-separated shocks. This confirms the main assumption of the phenomenological theory presented above. It follows from Figs. 1–4 and relation (12) that the anomaly in the high-order moments results only from the slow (algebraic) decrease of the PDF in the interval $\Delta u < 0$. As was pointed out above, in this case one expects a cutoff at some $\Delta u \approx U_0$.

We have also investigated the problem (1), (2) driven by the white-in-time random forces with $D(k) \neq 0$ only for $k < 5$ and $D(k) \propto k^{-3/2}$ [6]. The outcome of the simulations in both cases revealed the algebraically decreasing $\mathcal{P}(\Delta u, r) \propto r/|\Delta u|^q$ for $\Delta u/(\Delta u)_{\rm rms} \ll -1$, with the exponent q, related to the functional form of $D(k)$. The former case of the large-scale driven Burgers equation was investigated in a recent paper by Bouchaud, Mézard, and Parisi [5] using a replica trick in the limit of the space dimensionality $d \to \infty$. Although the scaling of the moments of velocity differences obtained in Ref. [5] is the same as the one observed in our simulations, the shape of the PDF in the $1d$ case, numerically found by us, differs dramatically from $\mathcal{P}(\Delta u, r) = (1-r)\delta(\Delta u - r) + \beta r F(\Delta u/U_0)$, derived in Ref. [5]. Here $F(x)$ is a scaling function and β is a number. This means that the physical mechanisms responsible for the anomalous scaling in the one- and multi-dimensional systems are different and understanding of the transition between the two behaviors is an extremely interesting challenge. We plan to publish detailed theoretical and numerical investigations of the different cases of forcing functions elsewhere [6].

This work was supported by grants from ARPA and AFOSR. Stimulating discussions with R. H. Kraichnan, A. Migdal, S. Orszag, A. Polyakov, and Ya. Sinai are gratefully acknowledged.

[1] A. Chekhlov and V. Yakhot, Phys. Rev. E **51**, R2739 (1995).

[2] A. Kolmogoroff, C. R. (Dokl.) Acad. Sci. URSS **30**, 301 (1941); **32**, 16 (1941).

[3] J. M. Burgers, *The Nonlinear Diffusion Equation. Asymptotic Solutions and Statistical Problems* (Reidel, Dordrecht, 1974); J. Krug and H. Spohn, in *Solids Far From Equilibrium: Growth, Morphology and Defects,* edited by C. Godréche (Cambridge University Press, Cambridge, England, 1992).

[4] A. Polyakov (unpublished).

[5] J. P. Bouchaud, M. Mézard, and G. Parisi, Phys. Rev. E **52**, 3656 (1995).

[6] V. Yakhot and A. Chekhlov (unpublished).